Published in final edited form as:
J Comp Neurol. 2010 June 1; 518(11): . doi:10.1002/cne.22334.

Connections of the Auditory Brainstem in a Songbird, *Taeniopygia guttata*. I. Projections of Nucleus Angularis and Nucleus Laminaris to the Auditory Torus

Nils O.E. Krützfeldt, **Priscilla Logerot**, **M. Fabiana Kubke**, and **J. Martin Wild***
Department of Anatomy, Faculty of Medical and Health Sciences, University of Auckland, PB 92019 Auckland, New Zealand

Abstract

Auditory information is important for social and reproductive behaviors in birds generally, but is crucial for oscine species (songbirds), in particular because in these species auditory feedback ensures the learning and accurate maintenance of song. While there is considerable information on the auditory projections through the forebrain of songbirds, there is no information available for projections through the brainstem. At the latter levels the prevalent model of auditory processing in birds derives from an auditory specialist, the barn owl, which uses time and intensity parameters to compute the location of sounds in space, but whether the auditory brainstem of songbirds is similarly functionally organized is unknown. To examine the songbird auditory brainstem we charted the projections of the cochlear nuclei angularis (NA) and magnocellularis (NM) and the third-order nucleus laminaris (NL) in zebra finches using standard tract-tracing techniques. As in other avian species, the projections of NM were found to be confined to NL, and NL and NA provided the ascending projections. Here we report on differential projections of NA and NL to the torus semicircularis, known in birds as nucleus mesencephalicus lateralis, pars dorsalis (MLd), and in mammals as the central nucleus of the inferior colliculus (ICc). Unlike the case in nonsongbirds, the projections of NA and NL to MLd in the zebra finch showed substantial overlap, in agreement with the projections of the cochlear nuclei to the ICc in mammals. This organization could suggest that the "what" of auditory stimuli is as important as "where."

Keywords

cochlear nuclei; central nucleus of inferior colliculus; MLd; zebra finch; avian

Birdsong plays an important role in a number of social and reproductive behaviors in passerine songbirds, including territorial defense, recognition of conspecifics, and courtship. As for speech in humans, the learning of birdsong during early development and its accurate maintenance during adulthood is critically dependent on auditory input from vocalizations emanating from conspecifics and self (Konishi, 1965; Nottebohm et al., 1976; Marler and Waser, 1977; Nordeen and Nordeen, 1992; Okanoya and Yamaguchi, 1997; Woolley and Rubel, 1997; Watanabe and Aoki, 1998; Leonardo and Konishi, 1999; Lombardino and Nottebohm, 2000; Cynx and von Rad, 2001). Consequently, considerable effort has been directed toward elucidating the sources of this auditory information and the route(s) by which it reaches telencephalic nuclei that control the species-specific song, via the descending projections of these nuclei on vocal motoneurons and respiratory premotor

*CORRESPONDENCE TO: Department of Anatomy, FMHS, University of Auckland, Auckland 1142, New Zealand. jm.wild@auckland.ac.nz.

neurons in the medulla (Nottebohm et al., 1976; Kelley and Nottebohm, 1979; Wild, 1993a,b, 1994; Fortune and Margoliash, 1995; Vates et al., 1996; Mello et al., 1998; Janata and Margoliash, 1999; Wild et al., 2000; Coleman and Mooney, 2004). However, no information is available for songbirds (which comprise about half the number of avian species) regarding the ascending projections of brainstem auditory nuclei, through which auditory information must pass to reach the forebrain. In nonsongbirds, such as pigeons and chickens, in which vocalizations are generally thought not to be learned (Konishi, 1965), the cochlear nuclei angularis (NA) and magnocellularis (NM) receive primary auditory afferents over the eighth nerve, NM projects bilaterally to nucleus laminaris (NL), and both NA and NL provide the ascending projections that innervate the superior olive, the lateral lemniscal nuclei, and finally the midbrain auditory torus, known as nucleus mesencephalicus lateralis, pars dorsalis (MLd) (Boord, 1968; Leibler, 1975; Conlee and Parks, 1986; Puelles et al., 1994; Wild, 1995). MLd and both the ventral and dorsal nuclei of the lateral lemniscus then project on nucleus ovoidalis (Ov) and nucleus parovoidalis (Ovp) of the dorsal thalamus, the former or both of which have been postulated to be homologous specifically with the ventral nucleus of the medial geniculate body of mammals (Karten, 1967, 1968; Wild, 1987).

In the barn owl—another nonsongbird, but in this case an auditory specialist with highly developed sound localizing skills (Payne, 1971; Knudsen et al., 1979)—the pattern of projections through NA, NM, and NL is generally similar to that in other nonsongbirds, but the specific pattern of terminations of NL and NA within the large central nucleus of the inferior colliculus (ICc; comparable to MLd in other species) forms distinct core (ICcc) and shells (ICcs) for the processing of time and intensity parameters, respectively (Knudsen, 1983; Takahashi and Konishi, 1988). The large, medial portion of MLd, which includes the NL-recipient core in this species (Takahashi and Konishi, 1988), and in some other birds of prey (Calford et al., 1985), is tonotopically organized (Knudsen and Konishi, 1978), and in the barn owl can be distinguished from the shell using acetylcholinesterase staining and calcium-binding protein immunohistochemistry (Takahashi et al., 1987; Adolphs, 1993; Wagner et al., 2003). Projections from the lateral shell converge on neurons in the external nucleus of IC (ICx), where a map of space around the animal is created. The barn owl has thus become the prevalent model for understanding the neural mechanisms underlying sound localization, which, unlike visual localization, can only be accomplished by a computation in the brain, and specifically by the processing of stimuli varying in the temporal and intensity domains (Konishi, 1995, 2003; Knudsen, 2002).

Unlike barn owls, zebra finches are rather poor at localizing auditory stimuli in the azimuthal plane (Park and Dooling, 1991), which in itself might pose a question about whether MLd is organized in a similar manner to MLd in the barn owl. Calcium-binding protein immunohistochemistry does appear to define core and shelf (sic? = shell) parts of MLd in this species (Braun et al., 1985, 1991), but the relation of this division to recent electro-physiological analyses of MLd is not clear. High frequencies are represented ventrally in MLd and lower frequencies dorsally, as they are in the barn owl ICc core (Woolley and Casseday, 2004), but whether this tonotopic organization is endowed by the projections of NL, as it is barn owls, or by those of NA, or a combination of both, is unknown. Moreover, an external nucleus comparable to that in the barn owl has not specifically been identified in zebra finches, or in any other avian species, either in terms of projections from a central MLd region or electrophysiologically in terms of a space map (Lewald, 1990). Leibler (1975) named an “external nucleus” in the pigeon, but this lies ventral, not rostrolateral, to MLd and is anatomically and functionally a somatosensory, not an auditory, nucleus (Wild, 1995, 1997).

In the auditory system, as in the visual and somatosensory systems, “what” is as functionally important as “where” (Alain et al., 2001; Diamond et al., 2008). Thus, in songbirds, because

of the importance of species-specific song, in general, and of the bird's own song, in particular (Doupe and Konishi, 1991; Janata and Margoliash, 1999; Coleman and Mooney, 2004) for the singing male and for the nonsinging but perceptive female, it may be that the "what" (i.e., the temporal and spectrotemporal acoustic pattern) of natural stimuli, particularly of song, is as important as the precise localization of "where" the song emanates (Casseday and Covey, 1996). Nevertheless, the ability to resolve acoustic patterns in vocalizations may well depend on the ability to localize the sound source accurately (Nelson and Suthers, 2004). In any case, certain acoustic features of songs and calls may be extracted differentially by different nuclei at different levels of the auditory brainstem (Hsu et al., 2004; Poirier et al., 2009). Given this possibility, it becomes particularly important to understand the details of the ascending auditory projections throughout the various stations of the auditory brainstem. In the present report we focus on the inputs to MLd, while the accompanying articles describe the inputs to the superior olive and nuclei of the lateral lemniscus (Krützfeldt et al., 2010) and the outputs of these nuclei (Wild et al., 2010).

MATERIALS AND METHODS

The experimental procedures were carried out according to the guidelines of the Animal Ethics Committee of the University of Auckland. Data from 55 adult (at least 100 days old, but exact age unknown) male zebra finches obtained from a local breeder were used for this study. For the tracing experiments, a total of 48 birds were anesthetized with an intramuscular injection of an equal parts mixture of ketamine (Parnell Laboratories, Auckland, New Zealand; 100 mg/kg) and xylazine (Rompun, Bayer; 20 mg/kg) and placed in a David Kopf stereotaxic frame (Kopf, Tujunga, CA) with the head tilted down 45° to the horizontal plane (Stokes et al., 1974). Injections of either biotinylated dextran amine (BDA; 10,000 MW, Invitrogen, Eugene, OR; 10%, in 1 M NaCl) and/or unconjugated cholera toxin B-chain (CTB; Sigma-Aldrich, St. Louis, MO; 1% in 0.1 M phosphate-buffered saline, pH 7.4) were made through glass micropipettes (outer diameter, 12–20 μm) by iontophoresis (2–4 μA positive current for 10–20 minutes). In different cases BDA and CTB were sometimes injected in the same bird on opposite sides of the brain, and sometimes on the same side.

The placement of stereotaxic injections was assisted by the use of electrophysiological identification of the auditory-responsive nuclei. Tungsten microelectrodes (Frederick Haer, Bowdoinham, NM; 2–4 Ω) were sometimes used initially to locate the nuclei by recording responses of single or multiple units to a variety of auditory stimuli. Signals were bandpass-filtered (300–5 kHz), amplified (AM 4-channel or AM 2-channel differential amplifiers, Models 1700 or 1800, respectively), and monitored with an oscilloscope and loud speaker. Once a nucleus had been located, the tungsten microelectrode was replaced by a tracer-filled glass pipette, through which recordings of auditory responses were subsequently made, prior to iontophoresis.

After a survival time of 3–4 days, the injected birds were deeply anesthetized and perfused through the heart with 0.9% saline followed by 4% paraformaldehyde (PFA, pH 7.4). The brains were blocked stereotaxically in the transverse or sagittal plane, cryoprotected in 30% sucrose overnight, and sectioned on a freezing microtome at 35 μm. Serial sections were collected in four or six series, all of which were used for the immunohistochemical visualization of either BDA or CTB, or both. All sections were preincubated in 50% aqueous methanol containing 1% H_2O_2. BDA was visualized using NeutrAvidin (Pierce Biotechnology, Rockford, IL) at a dilution of 1:1,000 in phosphate-buffered saline (PBS) plus 0.4% Triton X-100 for 1 hour, followed by the chromogen-solution (0.025% 3,3′-diamino-benzidine [DAB], 0.005% H_2O_2 and 0.015% $CoCl_2$ in PBS), which yielded a black reaction product. CTB was visualized using a goat anti-choleragenoid antibody (List

Biological Laboratories, Campbell, CA) diluted 1:30,000 overnight. This antibody was raised against purified choleragenoid and does not result in labeling following preabsorption of the antibody with excess concentration of choleragenoid (Stocker et al., 2006), and no labeling is seen in material where a CTB injection has not been performed (Kubke et al., 2004).

Incubation in the primary antibody was followed by a biotinylated rabbit antigoat antibody (Sigma-Aldrich) diluted 1:300 for 1 hour. NeutrAvidin diluted 1:1,000 was used to bind to the secondary antibody before incubation in the chromogen-solution, without $CoCl_2$, thereby yielding a brown reaction product. Parvalbumin (PV) immunoreactivity was visualized using a monoclonal anti-parvalbumin antibody (Swant clone 235, Basel, Switzerland) diluted 1:5,000 overnight. The antibody was produced by immunization of mice with parvalbumin purified from carp muscle, and hybridization of mouse myeloma cells with spleen cells from immunized mice. The antibody reacts specifically with PV in cultured nerve cells and in tissue originating from human, monkey, rabbit, rat, mouse chicken, and fish and specifically stains the 45Ca-binding spot of PV (MW 12.000) in a 2D immunoblot (Swant antibody specifications and Celio et al., 1988).

Incubation in this primary antibody was followed by biotinylated horse antimouse (Vector Laboratories, Burlingame, CA) diluted 1:300 for 1 hour. NeutrAvidin diluted 1:1,000 was used to bind to the secondary antibody before incubation in the chromogen solution. All incubations were carried out with agitation at room temperature and preceded by three 10-minute washes in PBS. For the visualization of the presence of Cytochrome C, animals were perfused with 0.9% saline through the heart, followed by 2.5% PFA and 0.5% glutaraldehyde in phosphate buffer, pH 7.4. Brains were postfixed for 6 hours and transferred to a solution containing 30% sucrose in PBS. Sections were cut coronally at 50 μm on a freezing microtome. Sections were then immersed in 90 mL 0.1 M PB containing 4 g sucrose, 27 mg Cytochrome C (Sigma), and 50 mg DAB for 2–4 hours in the dark (Wong-Riley, 1979). The reaction was stopped by washes in PBS. Sections were mounted on gelatin-coated slides. Every second series was counterstained with cresyl violet for the visualization of nuclear groups. Sections were dehydrated in ascending alcohols before coverslipping in DePeX (Serva, Heidelberg, Germany) from xylene. They were viewed using a Nikon Eclipse 80i light microscope and digitally photographed (5 megapixel resolution) prior to loading into Adobe Photoshop 5.5 software (Adobe Systems, San Jose, CA), which was used to adjust brightness, contrast, and off-section areas in accordance with journal policy. Some schematics were drawn with the aid of a macroprojector (Bausch and Lomb, Rochester, NY) or a camera lucida, and were then scanned into a personal computer for digital representation. Some other schematics and outlines of nuclear groups were drawn using CorelDraw12 (Ottawa, Canada) software on digitized Nissl-stained and uncounterstained sections.

RESULTS

Normal anatomy of NM, NA, and NL

The two cochlear nuclei (NA and NM) and NL lie close to each other as they straddle the dorsal and dorsolateral medullary-pontine junction. Although they overlap throughout much of their rostrocaudal extents, NL extends slightly more rostrally than either NA or NM. (Figs. 1, 10). In transverse, Nissl-counterstained sections, NA at caudal levels forms a triangular projection on the dorsolateral aspect of the free medulla (i.e., caudal to the level at which the cerebellum is attached to the hind-brain) and is separated from the underlying elongated NM by the root of the eighth nerve (Fig. 1A). Slightly more rostrally, just before the cerebellum starts to become attached to the brainstem, NA forms a humped, angular structure having lateral and medial parts with distinct cellular morphologies (Fig. 1B) (see

also NA in the pigeon: Häusler et al., 1999; and barn owl: Köppl, 2001; Soares et al., 2001). As NA extends rostrally the medial part becomes much larger than the lateral part and eventually becomes separated from it, so that at rostral levels two separate parts of NA can be seen in the same transverse section (Figs. 1C, 10), the medial part here comprising an ovoid collection of neurons situated dorsomedial to the tangential vestibular nucleus.

NM at caudal levels extends diagonally almost from the lateral periphery of the brainstem almost to the floor of the fourth ventricle (Fig. 1A). Here its neurons can clearly be seen to be arranged in rows running across the width of the nucleus, these rows presumably organized by incoming auditory nerve fascicles. More rostrally NM is more ovoid in cross section and lies more medially, under the floor of the fourth ventricle and medial to the NL, which here separates NM from NA (Fig. 1B). At its rostral pole NM is reduced to a few short vertical columns of neurons lying dorsolateral to the medial vestibular nucleus and medial to NL (Fig. 1C).

Throughout its rostrocaudal extent NL in transverse sections maintains a simple crescent shape having a medially facing concavity, but in sagittal sections it has dorsal, caudal, and rostral limbs. At caudal levels NL in transverse sections is composed of a single row of cells separating NA and NM, but at the junction of the three limbs seen in sagittal sections, NL is up to 20 cells wide (Figs. 1B, 10D, 11D). At levels caudal and rostral to this multilayered part of NL, the nucleus is surrounded by a clear region that contains the tufted dendrites of NL cell bodies and the axons of ipsilateral and contralateral NM projections to the internal and external aspects of NL, respectively (Fig. 1B,C). Surrounding this clear region is a conspicuous band of glia, thicker on the lateral aspect of NL, the curve of which is now also oriented almost vertically (Fig. 1C,D).

Normal anatomy of the torus semicircularis (MLd)

In zebra finches MLd has been defined by a variety of immunohistochemical markers (Braun, 1985, 1991; Watson et al., 1988) and in the greenfinch in the context of ascending somatosensory projections from the dorsal column nuclei to the intercollicular region, including the auditory torus (Wild, 1997). These various definitions are only partly congruent. Here we define MLd (Fig. 2) on the basis of its cytoarchitecture observed in Nissl-counter-stained sections, cytochrome oxidase staining, parvalbumin immunoreactivity, and as that portion of the torus in receipt of auditory projections from the brainstem auditory nuclei, whether or not it also receives somatosensory projections (Fig. 6; see also Wild, 1995). Thus, MLd in the zebra finch can be seen in transverse sections to form an irregular ovoid shaped nucleus oriented ventrolateral to dorsomedial under the tectal ventricle, and separated from it by a periventricular lamina (Puelles et al., 1994). A distinct, medially facing hilar region, which in some other species, e.g. pigeon (Karten and Hodos, 1967) and chicken (Puelles et al., 2007) transforms the ovoid-shaped nucleus into a kidney bean shape, is less obvious in the zebra finch MLd (Figs. 2, 6). As in greenfinches, pigeons, and chickens (Wild, 1997, 1995; Puelles et al., 1994), MLd in the zebra finch at caudal levels has a triangular dorsomedial extension toward the lateral corner of the fourth ventricle (Fig. 2), an extension previously and here called CM (caudomedial; Puelles et al., 1994) and shown to receive projection both from nucleus angularis and the dorsal column nuclei (Wild, 1995, 1997). Ventrally and ventrolaterally the curved borderline between MLd and the surrounding intercollicular region is often unclear in Nissl-counterstained sections. At more rostral levels, however, the dorsomedial border of MLd is straight-edged, where it abuts a core nucleus of the inter-collicular region (Puelles et al., 1994), commonly known as the dorsomedial nucleus (DM) (Fig. 2). This nucleus, which is part of the respiratory-vocal control system, projects on the medullary vocal motor nucleus and the premotor respiratory nuclei (Gurney, 1981; Wild, 2004; Wild et al., 1997), but no connection between DM and MLd has thus far been found. The neuropil of both MLd and DM is positive for parvalbumin

immunoreactivity (i.e., is PV-positive, Fig. 2), but whereas that of DM is derived from the projections of the telencephalic vocal control nucleus robustus arcopallialis (RA; Wild et al., 2001), that of MLd is not—thus explaining the absence of PV-positive neuropil in ICo of nonsongbirds, such as chickens, which do not have an RA (Zeng et al., 2008; Wild, 2008). Furthermore, many cell bodies of MLd in zebra finch are PV-positive, but those of DM are not (Fig. 2). Also at the level of DM, the ventromedial corner of MLd is cytoarchitecturally conspicuous and in cytochrome oxidase material is seen to form an almost separate subnucleus (see fig. 8B in Braun et al., 1985; Fig. 2D2, present study). But this subnucleus is considered part of MLd, since it receives projections from NA and NL and can be retrogradely labeled from injections of tracer into nucleus ovoidalis (Fig. 11F,G).

Tracing experiments

The proximity of NM, NA, and NL rendered their separate, confined injection a challenge, but we nevertheless considered it imperative that this challenge be met as well as possible in order to give proper credence to the resulting projections. Target accuracy and the ability to confine an injection to either NL or NA were sometimes enhanced by approaching the nuclei at an angle of some 20–25° from the vertical through the contralateral cerebellar hemisphere. The projections of NM, NA, and NL as defined here, then, are based on tracer injections that were confined to the target structure or to part thereof or, at most, included a small part of its immediate surround. (Figs. 3, 4; see Discussion for the importance of this inclusion, particularly with respect to NL). There was a trade-off between small injections completely confined to the nucleus that produced only very small or sparse terminal fields in MLd and somewhat larger injections that involved a part of the nuclear surround that produced terminal fields in MLd of an appreciable size and density. Injections in NM, however, often also encroached on the most medial edge of caudal NL. This we did not consider a problem because, although NM projects to NL bilaterally, NL projects neither to NM nor to the contralateral NL.

Projections of NM—Injections of BDA in NM (n = 5), an example of which is shown in Fig. 3, produced a complicated pattern of anterograde and retrograde labeling. Note first that the injection produced labeled fibers in the eighth nerve and a terminal field in the ipsilateral NA (Fig. 3). These terminations were assumed to have arisen from cochlear ganglion cells, which innervate NA and NM via axon collaterals (Cajal, 1908; Carr and Boudreau, 1991; Köppl, 1994, 2001). (Injections in NA did not retrogradely label NM cell bodies, see below.) In the case shown in Fig. 3, the terminations in NA were largely restricted to the medial part of the nucleus, where lower frequencies are known to be represented in NA of other songbirds (Konishi, 1970). This is probably consistent with the ventral location of the NM injection, where lower frequencies are likely represented at this rostrocaudal level. Note second that despite the fact that the NM injection encroached on the medial part of NL, retrogradely labeled cell bodies in the contralateral NM were not present at the same level, but at a more caudal level, which is not shown; that is, projections of NM to the contralateral NL do not cross the midline strictly in the stereotaxic transverse plane. Although a topographic organization of the NM to NL projections was not defined anterogradely by NM injections in the present study, it was strongly suggested by bilateral retrograde labeling of different clusters of NM neurons resulting from injections in different parts of NL (see below). Note third that NM injections produce intense fiber and terminal labeling throughout both the ipsilateral and contralateral NL (Fig. 3). While it was not possible to trace the course of individual fibers to their specific destination, it is clear that fibers originating from the NM of both sides and destined for the contralateral NL cross the midline in a commissure dorsal to the medial longitudinal fasciculus. In the barn owl and chicken it is known that these commissural fibers enter NL from its lateral or external aspect, whence they terminate primarily on NL dendrites (Parks and Rubel, 1975; Carr and Konishi, 1990).

Fibers entering NL from its medial or internal aspect originate from the ipsilateral NM. In Fig. 3, therefore, the labeled fibers between the unlabeled NM and the medial or internal aspect of NL may be axons of retrogradely labeled NM cells bodies lying caudal to the plane of section; and the labeled fibers medial to the unlabeled NM may be collateral axons of NM neurons destined for the contralateral NL.

In some cases a few labeled fibers from the NM injection descended through the ipsilateral tegmentum, but since these fibers took the course of NL axons (see below), it was concluded that they arose from the few medial NL cell bodies inadvertently included in the NM injection. NM neurons were not retrogradely labeled from any of the injections made in this study, other than those in NL (see below).

Projections of NA—Injections of either BDA or CTB into NA (n = 16; e.g., Figs. 4, 6) produced fiber and/or terminal and/or retrograde cell body labeling in a host of structures, some of which project to, rather than from, NA, thereby potentially complicating the interpretation of the orthograde projections. Injections in NA labeled fibers in the eighth nerve and retrogradely labeled cell bodies in the cochlear ganglion, which project to both NA and NM via axon collaterals (Fig. 5A). Fiber and terminal label was therefore present in the ipsilateral NM, with the latter of the calyceal type on NM cell bodies (Fig. 5B). Fiber and terminal labeling was also present in the contralateral NA, but there were no retrogradely labeled cell bodies there. Two sources of this contralateral labeling are likely: one the superior olive and the other the ventral nucleus of the lateral lemniscus (LLV), cell bodies in both of which were retrogradely labeled bilaterally from the NA injections (see below). Cells in these nuclei may, therefore, innervate NA (and NM and NL) bilaterally via branched axons (see Wild et al., 2009, 2010).

A consistent finding across all cases with injections in NA was that a small number of labeled fibers left the injection area ventrally from the most lateral aspect of the medulla to thread their way through the eighth nerve rootlets and descend throughout the lateral and ventrolateral margin of the tegmentum (not shown). These fibers provided scattered terminations to these regions of the medulla, particularly ventrolaterally, but they were not in continuity with terminations in the more rostrally situated superior olive. The specific origin of these lateral medullary terminations has not been determined and the region has not hitherto been regarded as auditory. However, injections of tracer into MLd retrogradely labeled a small cluster of neurons specifically in this ventrolateral portion of the medulla (see below).

Most NA axons (possibly accompanied by axons of some cells projecting to NA) traveled medially from the nucleus, dorsal to the eighth nerve root. At or before the point at which they met the lateral wall of glia that surrounds NL, they turned ventrally through several rostrocaudal levels, possibly corresponding to their level of exit from the nucleus (Fig. 5C). They then formed swaths of ventrally and ventrolaterally directed fibers in the lateral tegmentum as they approached the superior olive (OS, Fig. 5D). The pattern of input to the OS and to the nuclei of the lateral lemniscus is described in a separate article (Krützfeldt et al., 2010), but here it can be noted that while some NA axons terminated in the ipsilateral OS, others passed dorsal to it en route to the contralateral side through the ventral tegmentum. NA axons then traversed the lateral lemniscal nuclei to ascend through the midbrain medial to nucleus semilunaris and nucleus isthmi, pars parvocellularis (Ipc) before fanning out to enter MLd (Fig. 6). Some NA axons entered the ventrolateral border of MLd; other fibers made a right-angled bend laterally to access MLd from a horizontal direction through its medially facing surface, and many others turned through an acute-angled bend to enter MLd from a dorsomedial direction. In cases with larger injections of NA, fibers and terminations could be seen throughout MLd, with no region, including CM, being

systematically devoid of label. The ipsilateral MLd was innervated very sparsely, mostly in the mid-region of the nucleus. No labeling was observed rostral to MLd.

A topographic organization of the NA-MLd projection was clearly apparent when cases with medial NA injections were compared to cases with lateral NA injections (Fig. 6). These subtotal injections of NA resulted in terminal fields within MLd that were restricted to parts of the nucleus: medial NA injections (where lower frequencies are represented in other species; Konishi, 1970; Sachs and Sinnott, 1978; Köppl, 2001; Fukui and Ohmori, 2003) resulted in a terminal field largely restricted to dorsolateral MLd, while injections in lateral NA (where higher frequencies are represented in other species; Köppl, 2001; Fukuri and Ohmori, 2003), resulted in terminal fields confined to ventromedial MLd. A rostrocaudal topography was less clear-cut, but overall there was a tendency for the greatest density of terminations to lie within the caudal half of the nucleus.

Projections of NL—Injections of either BDA or CTB into NL (n = 24; e.g., Figs. 4, 7) produced fiber and terminal labeling in the ipsilateral and contralateral OS, the contralateral nuclei of the lateral lemniscus (Krützfeldt et al., 2010), and the ipsilateral and contralateral MLd. They also produced retrograde labeling of cell bodies in the ipsilateral and contralateral NM (see injections in NM, above), and ipsilateral and contralateral OS and LLV. NL injections also produced terminal labeling in NA, predominantly contralaterally and in the contralateral NM, which was of a noncalyceal type. This terminal labeling in NA and NM does not arise from NL, since injections in neither NA nor NM retrogradely labeled NL neurons (see above). The label likely derives from either OS and/or LLV neurons that innervate NL, NA, and NM (Wild et al., 2009, 2010).

Fibers labeled by NL injections left the nucleus directly from the ventrolateral aspect to head ventrolaterally toward the ipsilateral OS, thence to cross in the ventral tegmentum and traverse the nuclei of the lateral lemniscus. The trajectories of NL fibers entering MLd appeared similar to those of NA fibers (see above). Although total injections of NL could not be produced without significant involvement of other nuclei (the results of such injections not, therefore, being presented here), partial, confined injections of NL in different cases produced terminal fields that, together, appeared to account for the great majority of the volume of MLd, except CM (see above for NA projections) (Fig. 7). These terminal fields differed in density and in the volume of MLd labeled, but no region of MLd, except CM, appeared to be systematically devoid of fibers. Terminal fields resulting from several small injections into rostrolateral, rostromedial, caudolateral, and caudomedial NL together defined most of MLd, except CM, but did not reveal a topographic organization of the NL-MLd projection that could be discerned. As for NA, there was very sparse labeling in the ipsilateral MLd from NL injections and there was no labeling rostral to the midbrain. Terminal fields resulting from cases cut in the sagittal plane were largely confined dorsomedially in the nucleus at more rostral levels (Fig. 8). Overall, then, the greatest density of label in MLd from NL injections was in the rostral half of the nucleus, but this rostral predominance was not as pronounced as the caudal predominance of label resulting from NA injections. Furthermore, there was considerable overlap of NA and NL terminations throughout much of the nucleus (cf. Figs. 6, 7).

Dual injections—The overlap of NA and NL terminal fields in MLd that was apparent from cases with single injections was confirmed by dual injections of BDA and CTB into NL and NA, respectively, on the same side in 4 cases (Fig. 9). The terminal fields resulting from these injections in each case also overlapped to some extent in the ipsilateral OS and in the contralateral ventral (LLV) and intermediate (LLI) nuclei of the lateral lemniscus, but in the dorsal nucleus of the lateral lemniscus (LLD), the projections resulting from each of the two injections were confined to one or the other of the two separate LLD subdivisions

(LLDa or LLDp; see Wild, 1987, 1995; Krützfeldt et al., 2010). Together these cases support the conclusion drawn from the results of single injection cases (see above) that much, if not most, of MLd is innervated by both NA and NL. They also support the contention that the pattern of projections of NA and NL to MLd as described above cannot simply be accounted for by the injections in NA involving NL or vice versa (see Discussion).

Retrograde labeling resulting from MLd injections—To investigate the possibility of a cryptic topographic organization of the NA and NL projections to MLd, iontophoretic injections of CTB and/or BDA were made into different regions of MLd in a series of cases (n = 8; Fig.10). Because of the multiple ways in which MLd afferents enter and then run through the nucleus, however, many injections potentially involve fibers of passage. This is especially so for ventrolaterally or ventromedially located injections, which may interrupt many fibers entering either from below or through the medially facing aspect of the nucleus, respectively, and destined for other parts of MLd. Nevertheless, the pattern of retrograde labeling generally supported the results derived from anterograde tracing from NA and NL, particularly with respect to mediolateral regions of NA. For instance, CTB injections centered dorsally in MLd (e.g., Fig. 10A,B,D) retrogradely labeled neurons throughout medial NA but labeled few neurons in lateral NA. Injections in ventral MLd (e.g., Fig. 10F), on the other hand, labeled neurons in lateral NA, as well as neurons in medial NA, the latter possibly via fibers of passage. Neurons in NL, however, were labeled by all MLd injections, particularly those located rostrally (Fig. 10F), dorsally (Fig. 10D), or dorsomedially (Fig. 10C). A rostrocaudal topography of retrograde labeling was not clear, although the most rostral injection in MLd labeled the most NL neurons in the rostral pole of the nucleus (Fig. 10F). In one case receiving dual injections in MLd, a CTB injection was centered dorsolaterally (Figs. 10A, 11A) and a BDA injection was centered rostrally and dorsomedially, 300 μm further rostrally (Figs. 10E, 11B). The CTB injection labeled neurons throughout medial NA and a few in mid-rostrocaudal levels of NL (Fig. 10A), while the BDA injection labeled neurons mostly in NL, with a few in rostral NA (Figs. 10E, 11D). These results suggest that NL's terminal field in MLd preferentially includes its dorsomedial region at rostral levels, while NA's terminal field includes both dorsomedial and dorsolateral regions. Together the results of injections in different regions of MLd reinforce retrogradely the conclusion drawn from the anterograde tracing studies of NA and NL projections, namely, that there is substantial overlap of the projections of NA and NL to MLd throughout much of the nucleus, albeit with different concentrations of NA and NL terminations at different rostrocaudal levels.

Large injections in MLd retrogradely labeled a small cluster of neurons at the lateral edge of the brainstem at the level of the eighth nerve root (not shown). They lay in a similar location to the ventral extent of fibers and terminations produced by injections in NA (see Projections of NA, above).

DISCUSSION

Technical considerations

Despite the proximity of the cochlear nuclei and NL, we were able to produce injections that were centered on and largely confined to each of the nuclei in a sufficient number of cases to provide confidence in the pattern of projections as presented here. However, an unexpected finding was that some axons leaving NA approximated the glial boundary of NL as they turned ventrally to descend through the lateral tegmentum. Consequently, injections in NL that infringed on this boundary inadvertently could, and presumably did, label NA axons as fibers of passage. This was determined by inspecting every section through the cochlear

nuclei in cases receiving NL injections and counting the total number of neurons retrogradely labeled in NA. This number varied from 0–23 over the 24 cases, with 11 cases having fewer than 10 retrogradely labeled NA neurons. The effect of this unavoidable labeling on the pattern of terminations in MLd could not be quantified, but we feel that it is highly unlikely to change the general conclusion of substantial overlap of the NA and NL projections. Importantly, this conclusion is particularly supported by the results of the double injections in a small number of cases, which showed that the NA and NL terminal fields always overlapped to some extent within MLd, although they were largely separate in LLDa and LLDp, respectively (see Krützfeldt et al., 2010). We suggest that this dissociation could not have arisen had there been substantial contamination of the NA projections by the NL injections.

Nuclear projection patterns

The results of injections in NM caused no surprises in suggesting that the great majority, if not all, projections were to NL bilaterally, consistent with most findings in pigeons, chickens, and barn owls (Boord, 1968; Parks and Rubel, 1975; Takahashi and Konishi, 1988; Wild, 1995). Boord (1968), however, traced degenerating axons from the lateral part of NM in pigeons to the contralateral lemniscal nuclei, and Leibler (1975), also in pigeons, found a few retrogradely labeled cells in lateral and ventrolateral parts of contralateral NM following a large injection of horseradish peroxidase (HRP) in MLd in one out of 13 cases. In the zebra finch we also observed a few labeled fibers descending from the site of injection in NM, but we interpret this as inadvertent labeling of a few medial NL neurons. Neither MLd injections in the present study nor lateral lemniscal nuclear injections in a companion article (Krützfeldt et al., 2010) retrogradely labeled any NM neurons. We did find, however, that focused and subtotal injections of tracer into NL revealed clear-cut subtotal retrograde labeling of specific clusters of NM neurons on each side of the brain, suggesting a topographic organization of the NM projections, as described in chickens (Parks and Rubel, 1975) and barn owls (Takahashi and Konishi, 1988). Injections of tracer into either the entering eighth nerve or into NA also resulted in calyceal-type endings on NM cell bodies, either by axonal uptake and orthograde transport or by somatopetal transport to and somatofugal transport from neurons in the cochlear ganglion that project to NA and NM via branched axons (see also Takahashi and Konishi, 1988; Köppl, 1994, 2001).

The projections of NA and NL to MLd, however, were similar in some respects but different in others from previous results in other species, possibly reflecting differences in tracing technique, but also reflecting real differences in patterns of projection. Using silver degeneration methods following lesions of NA and NL in pigeons, Leibler (1975) found both nuclei to project only to the contralateral MLd, but other studies in both pigeons and other species have observed a small ipsilateral terminal field in MLd as well (Arends, 1981; Correia et al., 1982; Conlee and Parks, 1986; Wild, 1995; present study). Leibler (1975) found that the projections of NA were concentrated caudally in MLd, while those of NL were concentrated in and confined to rostromedial parts of MLd. This NL projection to rostromedial MLd in pigeons was confirmed by Wild (1995), using CTB-HRP as a tracer, but the projections from NA were found to be much more extensive throughout MLd, although they did not overlap those of NL. Conlee and Parks (1986) in chickens also found the projections of NA and NL to be segregated in MLd, but the projection of NL was confined to a medial part of MLd at caudal levels of the nucleus, while the ipsilateral projection from NA was confined to the rostral pole of MLd, resembling the contralateral projection of NL in pigeons. (This pattern of projections of NL and NA to MLd in chickens has been confirmed by Krützfeldt and Wild, unpubl. obs.)

The functional implications of these interspecies differences in the pattern of NA and NL projections to MLd are unclear. In the barn owl, however, the projections of NA and NL to

MLd have provided the scaffolding for an influential model of information processing related to sound localization (Konishi, 1995, 2003; Knudsen, 2002). In this species NM neurons code for the phase of ipsilateral auditory inputs (Sullivan and Konishi, 1984) and, by way of the bilateral and tonotopic projections to NL, originate a channel for the computation of interaural differences in the timing of sounds from the two ears (Carr and Konishi, 1990). NA, on the other hand, responds to and codes for ipsilateral auditory input having a wide range of intensities or levels (Sullivan and Konishi 1984; Köppl and Carr, 2003). The projections of NL and NA to the large MLd, or central nucleus of the inferior colliculus (ICc), as it is more commonly known in barn owls (as in mammals), are purely contralateral and terminate in largely nonover-lapping zones (as they do in chickens also; Conlee and Parks, 1986). The projection of NL is to a tonotopically organized, rostromedial, calretinin-positive “core” (Takahashi et al., 1987; Kubke et al., 1999; Wagner et al., 2003), in which projections from the caudal, low-frequency regions of NL terminate in dorsal regions of the core, while projections from more rostral, high-frequency regions of NL terminate in ventral regions of the core. Furthermore, there is a continuous dorsoventral mapping of frequencies throughout the core (Knudsen and Konishi, 1978; Wagner et al., 1987; Takahashi and Konishi, 1988). The projections of NA occupy all regions of ICc not occupied by the NL projection, thereby forming a “shell” around the NL terminal field (Takahashi and Konishi, 1988). Thus, within the barn owl’s ICc, time and intensity pathways occupy separate core and shell terminal zones, respectively. The two pathways converge, however, in the lateral shell, from where projections reach the external nucleus of IC (ICx) (see Fig. 1 in Carr et al., 1989). Here a map of auditory space is formed for the detection of the directions from which sounds originate (Knudsen and Konishi, 1978; Konishi, 2003).

The present findings are apparently different from those of previous tracing studies of NA and NL projections in nonsongbirds (Leibler, 1975; Conlee and Parks, 1986; Takahashi and Konishi, 1988; Wild, 1995) in that they demonstrate extensive overlap of NL and NA projections throughout much, if not most, of MLd. We found that the NL projections in the zebra finch did not form a “core” in MLd, but were diffusely distributed throughout the nucleus, although with a tendency to predominate in the rostral half of the nucleus. Moreover, we did not observe clear-cut differences in the rostrocaudal distribution of NL terminations in MLd from injections distributed in different rostrocaudal regions of NL—implying either an absence of frequency-specific projections to different rostrocaudal levels of MLd, or a weakly organized pattern of projections to MLd.

Nevertheless, a tonotopic organization of MLd is present in the zebra finch, as demonstrated electrophysiologically by Woolley and Casseday (2004), but the present study shows that this organization derives from the projections of NA rather than from those of NL. This tonotopy resembles that found in barn owls and other birds and mammals in that low frequencies are represented dorsally and high frequencies ventrally (Covey and Carr, 2005). In the zebra finch in the present study, the NA projections were found throughout the dorsoventral extent of MLd, “filling in,” as it were, between the high and low frequency domains found by Woolley and Casseday (2004). Although this could suggest that there is, in fact, a systematic gradation of frequency-specific terminal field densities throughout the depth of MLd, findings of discontinuities in the tonotopic sequence throughout the ICc of some avian and mammalian species suggest caution in this respect (Calford et al., 1985; Calford, 1988; Malmierca et al., 2008). In the zebra finch the NA terminal fields within in MLd derive from different parts of NA: injections in lateral NA, where higher-frequency sounds are coded in other songbirds (Konishi, 1970; Sachs and Sinnott, 1978) and barn owls (Köppl, 2001), labeled ventral regions of MLd, while injections in medial NA, where lower-frequency sounds are coded (Konishi, 1970; Sachs and Sinnott, 1978; Köppl, 2001), labeled dorsal regions of MLd, in accordance with the findings of Woolley and Casseday (2004).

Functional implications

The success of the barn owl model might have limited speculation about how the midbrain might process its ascending inputs for purposes other than sound localization (Scheich et al., 1977; Casseday and Covey, 1996; Hsu et al., 2004). Unlike the case of the barn owl, the ability of birds with small heads to localize sounds in the azimuthal plane has generally been considered relatively poor, the zebra finch in particular (Klump et al., 1986; Park and Dooling, 1991; Klump, 2000). There are, however, some notable exceptions that are almost as good as barn owls and that therefore challenge our understanding of the mechanisms used in sound localization in small-headed birds (Lewald, 1987; Nelson and Stoddard, 1998; Nelson and Suthers, 2004; Larsen et al., 2006). Furthermore, by analogy with the visual system, the ability to resolve acoustic detail may be dependent on the ability to localize the sound source (Nelson and Suthers, 2004). In the case of songbirds this means that accuracy of song recognition based on the resolution of spectral and intensity features of conspecific song will vary with the ability to localize the singer's voice in space. To the extent that this is the case in zebra finches, the NA and NL inputs to MLd in this species may render the functional organization of MLd different from that of ICc in barn owls.

In songbirds, acoustic feature extraction has traditionally been thought to be first or primarily performed at forebrain levels where song is perceived and analyzed in higher auditory areas to form the basis of song recognition and auditory-vocal learning and performance (Sen et al., 2001; Grace et al., 2003). Nevertheless, MLd neurons in the zebra finch have been shown to be already more selective for natural-like sounds than for other complex but synthetic sounds (Hsu et al., 2004; Poirier et al., 2009), even though higher auditory areas such as Field L and the caudomedial nidopallium (NCM) are progressively more selective for natural sounds. Moreover, Woolley and Casseday (2004, 2005) have shown that, as in the midbrain of chickens (Coles and Aitken, 1979), guinea fowl (Scheich et al., 1977), and bats and frogs (reviewed in Casseday and Covey, 1996), MLd neurons in the zebra finch have specialized tuning properties that are likely involved in the perception of complex acoustic signals such as occur in conspecific vocalizations (Woolley and Casseday, 2004, 2005; Logerot et al., 2009). MLd neurons have few specialized frequency tuning properties, they are relatively insensitive to changes in intensity, and many have onset responses suggestive of a role in the temporal processing of the acoustic features of songs and calls. But the responses of single MLd neurons do not code for song; rather, the synchronized responses of populations of MLd neurons "create a neural representation of the temporal patterns of songs" (Woolley et al., 2006, p. 2510). How neuronal properties are encoded at the level of single cells, or how populations of cells in the songbird MLd code for song, is not known, but it may be that a prerequisite for the coding of song, as for the encoding of space in the barn owl (Konishi, 2003), is input from more than one auditory center, either onto single MLd neurons, or at least onto the same MLd "cluster" or "module." In the zebra finch these inputs include not only those reported here from NA and NL, but also those from the OS, from two of three nuclei of the lateral lemniscus, and from the contralateral MLd (Krützfeldt et al., 2010). Some descending inputs to peripheral regions of MLd arise from the arcopallium, which, in turn, possibly relays descending signals from higher regions of the auditory telencephalon (Wild et al., 1993; Mello et al., 1998). Clearly, more refined and detailed anatomical studies of all these inputs onto MLd neurons are required to determine the degree of convergence, the influence of one input relative to others on the responses of MLd output neurons, and the intrinsic microcircuitry of MLd (cf. Oliver, 2005).

Comparison with mammals

Although it has been suggested that birds and mammals developed the capacity to hear airborne sounds independently at different times (Clack, 1997; Grothe, 2003), the detailed

effects of this on the differential evolution of central auditory systems in different taxa are unclear. Traditionally, NM in birds has been considered equivalent to the anteroventral cochlear nucleus (AVCN) of mammals, and NA to the posterior ventral cochlear nucleus (Boord and Rasmussen, 1963; Boord, 1968), but the bushy cells that make up NM in birds are similar morphologically and functionally to only one type of cell in the heterogeneous AVCN (Jhaveri and Morest, 1982; Sullivan and Konishi, 1984; Cant and Benson, 2003). NL, to which NM projects bilaterally, has been compared to the medial superior olive (MSO) of mammals, because it is the first site of bilateral input to an interaural time difference (ITD) pathway that, in some birds, at least, functions according to a model of coincidence detection (Jeffress, 1948; Hyson, 2005). The ITD circuitry in mammals and birds, however, involves different forms of inhibition with different postsynaptic and functional effects (feedforward and glycinergic to the MSO in mammals, versus feedback and GABAergic to NL in birds) (Grothe, 2003). Moreover, these inhibitory projections have origins in different brainstem auditory nuclei in the two classes: the medial nucleus of the trapezoid body (MNTB) and the lateral superior olivary nucleus (SON) in mammals and the OS in birds. Despite a similarity in name, therefore, the OS of birds is unlikely to be homologous with the LSO (or the MNTB) of mammals (Grothe, 2003). Nevertheless, NL and the MSO both project to the MLd/ICc, although the projections of NL are contralateral, whereas those of MSO are ipsilateral. The projections of NL and NA to the contralateral MLd are distinctly similar to those of the anterior and posterior ventral cochlear nuclei to the contralateral ICc in mammals in that their terminal fields overlap substantially (Osen, 1972; Cant, 2005; Cant and Benson, 2008; present results). Also, as for the projections of NA to MLd in the zebra finch, those of the cochlear nuclei to ICc in cats and gerbils are topographic and tonotopic, with low frequencies represented dorsally and high frequencies ventrally. As in birds, the cochlear projections in mammals are predominantly contralateral, but there appear to be more ipsilateral projections as well, at least in some mammals. Other differences in the auditory pathways of birds and mammals include the absence of commissural projections between the cochlear nuclei in birds (the projection of NM to the contralateral NL, although commissural, is to a third-order nucleus), the absence of a dorsal cochlear nucleus in birds, and hence the absence of any projection from such a nucleus to the auditory thalamus—in contrast to the dorsal cochlear nuclear projections in mammals (Malmierca et al., 2002, 2005; Anderson et al., 2006, 2009)—and the absence of projections to the pontine and mesencephalic reticular formation, at least those that are similar to those in various mammals (Cant and Benson, 2003). A sparse projection to the rostrolateral medulla that possibly arises from NA was found in the present study, and cells receiving this projection may project to MLd, but these projections require further retrograde and anterograde confirmation before they can be accepted as part of the ascending auditory system.

In concluding, we emphasize two important points of comparison. First, one suggestion resulting from the present studies in comparison with those in mammals is that the organization of the projections from NA and NL to the auditory midbrain in species such as barn owls, pigeons, and chickens may be characteristic of nonsongbirds in general. Although this may have been assumed, these three groups of birds belong to widely differing lineages, with owls now being grouped with passerines (which include songbirds) (Hackett et al., 2008). Thus, many more species from different lineages would need to be examined to corroborate this assumption. Meanwhile, the presence and functional significance of alternative organizations of MLd, e.g., one in which the NA and NL projections are not distinctly separate, as in songbirds, has not hitherto been realized. To the extent that the organization of the NA and NL projections to MLd in zebra finches is representative of that in songbirds in general, then the organization in about half the number of avian species, at least, will have a distinct similarity to that in mammals. To what extent the synaptic,

intrinsic, and functional organization of MLd in songbirds is similar to that in the central nucleus of the IC in mammals remains to be determined (cf. Oliver, 2005).

Second, one theory of the function of the inferior colliculus in mammals (Casseday and Covey, 1996) has emphasized its involvement in the motor control of auditorily elicited fixed action patterns. An extension to birds was made by way of the example of head turning in barn owls, which can be elicited by sounds of prey at highly specific loci (Knudsen et al., 1979). This accurate motor behavior is mediated through the projections of the ICx to the optic tectum, and from there to bulbospinal neurons in the medial pontine tegmentum (Knudsen and Knudsen, 1983; Masino and Knudsen, 1992). However, we know of no other behavior of birds that has been shown to be mediated by projections from the IC to brainstem premotor neurons. An obvious candidate is vocalization, especially as this plays such a significant part in Casseday and Covey's theory, as well as being the basis of the present study, but a projection from ICc to the adjacent respiratory-vocal control nucleus of the intercollicular complex (DM), or to any other brainstem premotor nucleus, or to the cerebellum, has thus far not been found in birds in general or songbirds in particular (Wild et al., 1997; present results). Other points of comparison with respect to the control of avian and mammalian vocalizations are made in Krützfeldt et al. (2010). The point is that there is no anatomical evidence thus far that the ICc of birds other than barn owls is involved in the sensorimotor control of anything resembling a fixed action pattern, at least not by way of projections to the brainstem. Rather the ICc, at least in songbirds, seems very much dedicated to the analysis of biologically important sounds (Woolley and Casseday, 2004, 2005), such as the complex vocalizations of conspecifics (in agreement with Casseday and Covey's [1996] theory) (Logerot et al., 2009), but this analysis seems mainly to serve the cognitive requirements of the forebrain not only in song learning but also in song production, by way of the projections of the ICc to the auditory thalamus and finally to the song control nuclei of the telencephalon (Wild, 2004, 2008).

Acknowledgments

We thank Silke Fuchs for technical assistance.

Grant sponsor: Royal Society of New Zealand Marsden Fund (to J.M.W.); Grant sponsor: National Institutes of Health (NIH); Grant number: R01 NS029467 (to R.A. Suthers and J.M.W.).

LITERATURE CITED

Adolphs R. Acetylcholinesterase staining differentiates functionally distinct auditory pathways in the barn owl. J Comp Neurol. 1993; 329:365–377. [PubMed: 7681456]

Alain C, Arnott SR, Hevenor S, Graham S, Grady CL. "What" and "where" in the human auditory system. Proc Natl Acad Sci U S A. 2001; 98:12301–12306. [PubMed: 11572938]

Anderson LA, Malmierca MS, Wallace MN, Palmer AR. Evidence for a direct, short latency projection from the dorsal cochlear nucleus to the auditory thalamus in the guinea pig. Eur J Neurosci. 2006; 24:491–498. [PubMed: 16836634]

Anderson LA, Izquierdo MA, Antunes FM. A monosynaptic pathway from dorsal cochlear nucleus to auditory cortex in rat. Neuroreport. 2009; 20:462–466. [PubMed: 19240662]

Arends, JJ. PhD Thesis. University of Leiden; Leiden, Netherlands: 1981. Sensory and motor aspects of the trigeminal system in the mallard (Anas Platyrhynchos L.).

Arends JJ, Zeigler HP. Anatomical identification of an auditory pathway from a nucleus of the lateral lemniscal system to the frontal telencephalon (nucleus basalis) of the pigeon. Brain Res. 1986; 398:375–381. [PubMed: 3801910]

Boord RL. Ascending projections of the primary cochlear nuclei and nucleus laminaris in the pigeon. J Comp Neurol. 1968; 133:523–541. [PubMed: 4185132]

Boord RL, Rasmussen GL. Projection of the cochlear and lagenar nerves on the cochlear nuclei of the pigeon. J Comp Neurol. 1963; 120:463–475. [PubMed: 14013817]

Braun K, Scheich H, Schachner M, Heizmann CW. Distribution of parvalbumin, cytochrome oxidase activity and 14C-2-deoxyglucose uptake in the brain of the zebra finch I. Auditory and vocal motor systems. Cell Tissue Res. 1985; 240:101–115.

Braun K, Scheich H, Heizmann CW, Hunziker W. Parvalbumin and calbindin-D28K immunoreactivity as developmental markers of auditory and vocal motor nuclei of the zebra finch. Neuroscience. 1991; 40:853–869. [PubMed: 2062443]

Calford MB. Constraints on the coding of sound frequency imposed by the avian interaural canal. J Comp Physiol [A] Neuroethol Sens Neural Behav Physiol. 1988; 162:491–502.

Calford MB, Wise LZ, Pettigrew JD. Coding of sound location and frequency in the auditory midbrain of diurnal birds of prey, families accipitridae and falconidae. J Comp Physiol [A] Neuroethol Sens Neural Behav Physiol. 1985; 157:149–160.

Cant, NB. Projections from the cochlear nuclear complex to the inferior colliculus. In: Winer, JA.; Schreiner, CE., editors. The inferior colliculus. Springer; New York: 2005. p. 115-131.

Cant NB, Benson CG. Parallel auditory pathways: projection patterns of the different neuronal populations in the dorsal and ventral cochlear nuclei. Brain Res Bull. 2003; 60:457–474. [PubMed: 12787867]

Cant NB, Benson CG. Organization of the inferior colliculus of the gerbil: projections from the cochlear nucleus. Neuroscience. 2008; 154:206–217. [PubMed: 18359572]

Carr CE, Boudreau RE. Central projections of auditory nerve fibers in the barn owl. J Comp Neurol. 1991; 314:306–318. [PubMed: 1723997]

Carr CE, Konishi M. A circuit for detection of interaural time differences in the brainstem of the barn owl. J Neurosci. 1990; 10:3227–3246. [PubMed: 2213141]

Carr CE, Fujita I, Konishi M. Distribution of GABAergic neurons and terminals in the auditory system of the barn owl. J Comp Neurol. 1989; 286:190–207. [PubMed: 2794115]

Casseday JH, Covey E. A neuroethological theory of the operation of the inferior colliculus. Brain Behav Evol. 1996; 47:311–336. [PubMed: 8796964]

Celio MR, Baier W, Scharer L, de Viragh PA, Gerday C. Monoclonal antibodies directed against the calcium binding protein parvalbumin. Cell Calcium. 1988; 9:81–86. [PubMed: 3383226]

Clack JA. The evolution of tetrapod ears and the fossil record. Brain Behav Evol. 1997; 50:198–212. [PubMed: 9310195]

Coleman MJ, Mooney R. Synaptic transformations underlying highly selective auditory representations of learned birdsong. J Neurosci. 2004; 24:7251–7265. [PubMed: 15317851]

Coles RB, Aitken LM. The response properties of auditory neurons in the midbrain of the domestic fowl (*Gallus gallus*) to monaural and binaural stimuli. J Comp Physiol [A] Neuroethol Sens Neural Behav Physiol. 1979; 134:241–251.

Conlee JW, Parks TN. Origin of ascending auditory projections to the nucleus mesencephalicus lateralis pars dorsalis in the chicken. Brain Res. 1986; 367:96–113. [PubMed: 3697720]

Correia MJ, Eden AR, Westlund KN, Coulter JD. Organization of ascending auditory pathways in the pigeon (Columba livia) as determined by autoradiographic methods. Brain Res. 1982; 234:205–212. [PubMed: 7059826]

Covey, E.; Carr, CE. The auditory midbrain in bats and birds. In: Winer, JA.; Schreiner, CE., editors. The inferior colliculus. Springer; New York: 2005. p. 493-536.

Cynx J, Von Rad U. Immediate and transitory effects of delayed auditory feedback on bird song production. Anim Behav. 2001; 62:305–312.

Diamond ME, von Heimendahl M, Knutsen PM, Kleinfeld D, Ahissar E. 'Where' and 'what' in the whisker sensorimotor system. Nat Rev Neurosci. 2008; 9:601–612. [PubMed: 18641667]

Doupe AJ, Konishi M. Song-selective auditory circuits in the vocal control system of the zebra finch. Proc Natl Acad Sci U S A. 1991; 88:11339–11343. [PubMed: 1763048]

Fortune ES, Margoliash D. Parallel pathways and convergence onto HVc and adjacent neostriatum of adult zebra finches (Taeniopygia guttata). J Comp Neurol. 1995; 360:413–441. [PubMed: 8543649]

Fukui I, Ohmori H. Nucleus angularis of the chicken: developmental changes in membrane excitability and morphology of neurons. J Physiol. 2003; 548:219–232. [PubMed: 12576492]

Grace JA, Amin N, Singh NC, Theunissen FE. Selectivity for conspecific song in the zebra finch auditory forebrain. J Neurophysiol. 2003; 89:472–487. [PubMed: 12522195]

Grothe B. New roles for synaptic inhibition in sound localization. Nate Rev Neurosci. 2003; 4:540–550.

Gurney ME. Hormonal control of cell form and number in the zebra finch song system. J Neurosci. 1981; 1:658–673. [PubMed: 7346574]

Hackett SJ, Kimball RT, Reddy S, Bowie RCK, Braun EL, Braun MJ, Chojnowski JL, Cox WA, Han K-L, Harshman J, Huddleston CJ, Marks BD, Miglia KJ, Moore WS, Sheldon FH, Steadman DW, Witt CC, Yuri T. A phylogenomic study of birds reveals their evolutionary history. Science. 2008; 320:1763–1768. [PubMed: 18583609]

Häusler UH, Sullivan WE, Soares D, Carr CE. A morphological study of the cochlear nuclei of the pigeon (Columba livia). Brain Behav Evol. 1999; 54:290–302. [PubMed: 10640788]

Hsu A, Woolley SM, Fremouw TE, Theunissen FE. Modulation power and phase spectrum of natural sounds enhance neural encoding performed by single auditory neurons. J Neurosci. 2004; 24:9201–9211. [PubMed: 15483139]

Hyson RL. The analysis of interaural time differences in the chick brain stem. Physiol Behav. 2005; 86:297–305. [PubMed: 16202434]

Janata P, Margoliash D. Gradual emergence of song selectivity in sensorimotor structures of the male zebra finch song system. J Neurosci. 1999; 19:5108–5118. [PubMed: 10366643]

Jeffress LA. A place theory of sound localization. J Comp Physiol Psychol. 1948; 41:35–39. [PubMed: 18904764]

Jhaveri S, Morest DK. Neuronal architecture in nucleus magnocellularis of the chicken auditory system with observations on nucleus laminaris: a light and electron microscope study. Neuroscience. 1982; 7:809–836. [PubMed: 7099420]

Karten HJ. The organization of the ascending auditory pathway in the pigeon (Columba livia). I. Diencephalic projections of the inferior colliculus (nucleus mesencephali lateralis, pars dorsalis). Brain Res. 1967; 6:409–427. [PubMed: 6076249]

Karten HJ. The ascending auditory pathway in the pigeon (Columba livia). II. Telencephalic projections of the nucleus ovoidalis thalami. Brain Res. 1968; 11:134–153. [PubMed: 5749228]

Karten, HJ.; Hodos, W. A stereotaxic atlas of the brain of the pigeon (*Columba livia)*. Johns Hopkins Press; Baltimore, MD: 1967.

Kelley DB, Nottebohm F. Projections of a telencephalic auditory nucleus-field L-in the canary. J Comp Neurol. 1979; 183:455–469. [PubMed: 759444]

Klump, GM. Sound localization in birds. In: Dooling, RJ.; Fay, RR.; Popper, AN., editors. Comparative hearing: birds and reptiles. Vol. vol.13. Springer; New York: 2000. p. 380

Klump GM, Windt W, Curio E. The great tit's (*Parus major*) auditory resolution in azimuth. J Comp Physiol [A] Neuroethol Sens Neural Behav Physiol. 1986; 158:383–390.

Knudsen EI. Subdivisions of the inferior colliculus in the barn owl (Tyto alba). J Comp Neurol. 1983; 218:174–186. [PubMed: 6886070]

Knudsen EI. Instructed learning in the auditory localization pathway of the barn owl. Nature. 2002; 417:322–328. [PubMed: 12015612]

Knudsen EI, Konishi M. Space and frequency are represented separately in auditory midbrain of the owl. J Neurophysiol. 1978; 41:870–884. [PubMed: 681991]

Knudsen EI, Knudsen PF. Space-mapped auditory projections from the inferior colliculus to the optic tectum in the barn owl (*Tyto alba*). J Comp Neurol. 1983; 218:187–196. [PubMed: 6886071]

Knudsen EI, Blasdel GG, Konishi M. Sound localization by the barn owl (Tyto alba) measured with the search coil technique. J Comp Physiol [A] Neuroethol Sens Neural Behav Physiol. 1979; 133:1–11.

Konishi M. The role of auditory feedback in the control of vocalization in the white-crowned sparrow. Z Tierpsychol. 1965; 22:770–783. [PubMed: 5874921]

Konishi M. Comparative neurophysiological studies of hearing and vocalizations in songbirds. Z vergl Physiol. 1970; 66:257–272.

Konishi, M. Neural mechanisms of auditory image formation. In: Gazzaniga, MS., editor. The cognitive neurosciences. MIT Press; Boston: 1995. p. 269-277.

Konishi M. Coding of auditory space. Annu Rev Neurosci. 2003; 26:31–55. [PubMed: 14527266]

Köppl C. Auditory nerve terminals in the cochlear nucleus magnocellularis: differences between low and high frequencies. J Comp Neurol. 1994; 339:438–446. [PubMed: 8132870]

Köppl C. Tonotopic projections of the auditory nerve to the cochlear nucleus angularis in the barn owl. J Assoc Res Otolaryngol. 2001; 2:41–53. [PubMed: 11545149]

Köppl C, Carr CE. Computational diversity in the cochlear nucleus angularis of the barn owl. J Neurophysiol. 2003; 89:2313–2329. [PubMed: 12612008]

Krützfeldt NOE, Logerot P, Kubke MF, Wild JM. Connections of the auditory brainstem in a songbird, *Taeniopygia guttata*. II. Projections of nucleus angularis and nucleus laminaris to the superior olive and lateral lemniscal nuclei. J Comp Neurol. 2010; 518:2135–2148. [PubMed: 20394062]

Kubke MF, Gauger B, Basu L, Wagner H, Carr CE. Development of calretinin immunoreactivity in the brainstem auditory nuclei of the barn owl (*Tyto alba*). J Comp Neurol. 1999; 415:189–203. [PubMed: 10545159]

Kubke MF, Ross JM, Wild JM. Vagal innervation of the air sacs in a songbird, *Taenopygia guttata*. J Anat. 2004; 204:283–292. [PubMed: 15061754]

Larsen ON, Dooling RJ, Michelsen. The role of pressure difference reception in the directional hearing of budgerigars (*Melopsittacus undulatus*). J Comp Physiol [A] Neuroethol Sens Neural Behav Physiol. 2006; 192:1063–1072.

Leibler, LM. PhD Thesis. Massachusetts Institute of Technology; Cambridge, MA: 1975. Monaural and binaural pathways in the ascending auditory system of the pigeon.

Leonardo A, Konishi M. Decrystallization of adult bird-song by perturbation of auditory feedback. Nature. 1999; 399:466–470. [PubMed: 10365958]

Lewald J. Neural mechanisms of directional hearing in the pigeon. Exp Brain Res. 1990; 82:423–436. [PubMed: 2286242]

Logerot, P.; Wild, JM.; Kubke, MF. Auditory processing of conspecific vocalizations in the auditory midbrain of the zebra finch. Paper presented at the Australasian Winter Conference on Brain Research; Queenstown, New Zealand. August 29–September; 2009. p. 2

Lombardino AJ, Nottebohm F. Age at deafening affects the stability of learned song in adult male zebra finches. J Neurosci. 2000; 20:5054–5064. [PubMed: 10864963]

Malmierca MS, Merchan MA, Henkel CK, Oliver DL. Direct projections from cochlear nuclear complex to auditory thalamus in the rat. J Neurosci. 2002; 22:10891–10897. [PubMed: 12486183]

Malmierca MS, Saint Marie RL, Merchan MA, Oliver DL. Laminar inputs from dorsal cochlear nucleus and ventral cochlear nucleus to the central nucleus of the inferior colliculus: two patterns of convergence. Neuroscience. 2005; 136:883–894. [PubMed: 16344158]

Marler P, Waser MS. Role of auditory feedback in canary song development. J Comp Physiol Psychol. 1977; 91:8–16. [PubMed: 838918]

Masino T, Knudsen EI. Anatomical pathways from the optic tectum to the spinal cord subserving orienting movements in the barn owl. Exp Brain Res. 1992; 92:194–208. [PubMed: 1493861]

Mello CV, Vates GE, Okuhata S, Nottebohm F. Descending auditory pathways in the adult male zebra finch (Taeniopygia guttata). J Comp Neurol. 1998; 395:137–160. [PubMed: 9603369]

Nelson BS, Stoddard PK. Accuracy of auditory distance and azimuth perception by a passerine bird in natural habitat. Anim Behav. 1998; 56:467–477. [PubMed: 9787038]

Nelson BS, Suthers RA. Sound localization in a small passerine bird: discrimination of azimuth as a function of head orientation and sound frequency. J Exp Biol. 2004; 207(Pt 23):4121–4133. [PubMed: 15498958]

Nordeen KW, Nordeen EJ. Auditory feedback is necessary for the maintenance of stereotyped song in adult zebra finches. Behav Neural Biol. 1992; 57:58–66. [PubMed: 1567334]

Nottebohm F, Stokes TM, Leonard CM. Central control of song in the canary, Serinus canarius. J Comp Neurol. 1976; 165:457–486. [PubMed: 1262540]

Okanoya K, Yamaguchi A. Adult Bengalese finches (Lonchura striata var. domestica) require real-time auditory feedback to produce normal song syntax. J Neurobiol. 1997; 33:343–356. [PubMed: 9322153]

Oliver, DL. Neuronal organization in the inferior colliculus. In: Winer, JA.; Schreiner, CE., editors. The inferior colliculus. Springer; New York: 2005. p. 69-114.

Osen KK. Projection of the cochlear nuclei on the inferior colliculus in the cat. J Comp Neurol. 1972; 144:355–372. [PubMed: 5027335]

Park TJ, Dooling RJ. Sound localization in small birds: absolute localization in azimuth. J Comp Psychol. 1991; 105:125–133. [PubMed: 1860306]

Parks TN, Rubel EW. Organization and development of brain stem auditory nuclei of the chicken: organization of projections from n. magnocellularis to n. laminaris. J Comp Neurol. 1975; 164:435–448. [PubMed: 1206128]

Payne RS. Acoustic location of prey by barn owls (Tyto alba). J Exp Biol. 1971; 54:535–573. [PubMed: 5090092]

Poirier C, Boumans T, Verhoye M, Balthazart J, Van der Linden A. Own-song recognition in the songbird auditory pathway. J Neurosci. 2009; 29:2252–2258. [PubMed: 19228978]

Puelles L, Robles C, Martinez-de-la-Torre M, Martinez S. New subdivision schema for the avian torus semicircularis: neurochemical maps in the chick. J Comp Neurol. 1994; 340:98–125. [PubMed: 8176005]

Puelles, L.; Martínez-de-la-Torre, M.; Paxinos, G.; Watson, C.; Martínez, S. An atlas featuring neuromeric subdivisions and mammalian homologies. Elsevier, Academic Press; Amsterdam: 2007. The chick brain in stereotaxic coordinates.

Sachs MB, Sinnott JM. Responses to tones of single cells in nucleus magnocellularis and nucleus angularis of the redwing blackbird (*Agelaius phoeniceus*). J Comp Physiol [A] Neuroethol Sens Neural Behav Physiol. 1978; 126:347–361.

Scheich H, Langner G, Koch R. Coding of narrow-band and wide-band vocalizations in the auditory midbrain nucleus (MLD) of the guinea fowl (Numida meleagris). J Comp Physiol [A] Neuroethol Sens Neural Behav Physiol. 1977; 117:245–265.

Sen K, Theunissen FE, Doupe AJ. Feature analysis of natural sounds in the songbird auditory forebrain. J Neurophysiol. 2001; 86:1445–1458. [PubMed: 11535690]

Soares D, Carr CE. The cytoarchitecture of the nucleus angularis of the barn owl (Tyto alba). J Comp Neurol. 2001; 429:192–205. [PubMed: 11116214]

Stocker SD, Simmons JR, Stornetta RL, Toney GM, Guyenet PG. Water deprivation activates a glutamatergic projection from the hypothalamic paraventricular nucleus to the rostral ventrolateral medulla. J Comp Neurol. 2006; 494:673–685. [PubMed: 16374796]

Sullivan WE, Konishi M. Segregation of stimulus phase and intensity coding in the cochlear nucleus of the barn owl. J Neurosci. 1984; 4:1787–1799. [PubMed: 6737041]

Takahashi TT, Konishi M. Projections of the cochlear nuclei and nucleus laminaris to the inferior colliculus of the barn owl. J Comp Neurol. 1988; 274:190–211. [PubMed: 2463286]

Takahashi TT, Carr CE, Brecha N, Konishi M. Calcium binding protein-like immunoreactivity labels the terminal field of nucleus laminaris of the barn owl. J Neurosci. 1987; 7:1843–1856. [PubMed: 2439666]

Vates GE, Broome BM, Mello CV, Nottebohm F. Auditory pathways of caudal telencephalon and their relation to the song system of adult male zebra finches. J Comp Neurol. 1996; 366:613–642. [PubMed: 8833113]

Wagner H, Takahashi T, Konishi M. Representation of interaural time difference in the central nucleus of the barn owl's inferior colliculus. J Neurosci. 1987; 7:3105–3116. [PubMed: 3668618]

Wagner H, Güntürkün O, Nieder B. Anatomical markers for the subdivisions of the barn owl's inferior-collicular complex and adjacent peri- and subventricular structures. J Comp Neurol. 2003; 465:145–159. [PubMed: 12926022]

Watanabe A, Aoki K. The role of auditory feedback in the maintenance of song in adult male Bengalese finches Lonchura striata var. domestica. Zool Sci. 1998; 15:837–841.

Watson JT, Adkins-Regan E, Whiting P, Lindstrom JM, Podleski TR. Autoradiographic localization of nicotinic acetylcholine receptors in the brain of the zebra finch (Poephila guttata). J Comp Neurol. 1988; 274:255–264. [PubMed: 3209741]

Wild JM. Nuclei of the lateral lemniscus project directly to the thalamic auditory nuclei in the pigeon. Brain Res. 1987; 408:303–307. [PubMed: 2439168]

Wild JM. The avian nucleus retroambigualis: a nucleus for breathing, singing and calling. Brain Res. 1993a; 606:319–324. [PubMed: 8387862]

Wild JM. Descending projections of the songbird nucleus robustus archistriatalis. J Comp Neurol. 1993b; 338:225–241. [PubMed: 8308169]

Wild JM. The auditory-vocal-respiratory axis in birds. Brain Behav Evol. 1994; 44:192–209. [PubMed: 7842281]

Wild JM. Convergence of somatosensory and auditory projections in the avian torus semicircularis, including the central auditory nucleus. J Comp Neurol. 1995; 358:465–486. [PubMed: 7593743]

Wild JM. The avian somatosensory system: the pathway from wing to Wulst in a passerine (Chloris chloris). Brain Res. 1997; 759:122–134. [PubMed: 9219870]

Wild JM. Functional neuroanatomy of the sensorimotor control of singing. Ann N Y Acad Sci. 2004; 1016:438–462. [PubMed: 15313789]

Wild, JM. Neuroscience of bird-song. Cambridge University Press; Cambridge, UK: 2008. Birdsong: anatomical foundations and central mechanisms of sensorimotor integration; p. 136-151.

Wild JM, Karten HJ, Frost BJ. Connections of the auditory forebrain in the pigeon (Columba livia). J Comp Neurol. 1993; 337:32–62. [PubMed: 8276991]

Wild JM, Li D, Eagleton C. Projections of the dorsome-dial nucleus of the intercollicular complex (DM) in relation to respiratory-vocal nuclei in the brainstem of pigeon (Columba livia) and zebra finch (Taeniopygia guttata). J Comp Neurol. 1997; 377:392–413. [PubMed: 8989654]

Wild JM, Williams MN, Suthers RA. Neural pathways for bilateral vocal control in songbirds. J Comp Neurol. 2000; 423:413–426. [PubMed: 10870082]

Wild JM, Williams MN, Suthers RA. Parvalbumin-positive projection neurons characterise the vocal premotor pathway in male, but not female, zebra finches. Brain Res. 2001; 917:235–252. [PubMed: 11640910]

Wild JM, Krützfeldt NOE, Kubke MF. Afferents to the cochlear nuclei and nucleus laminaris from the ventral nucleus of the lateral lemniscus in the zebra finch (*Taeniopygia guttata*). Hear Res. 2009; 212:3119–3124.

Wild JM, Krützfeldt NOE, Kubke MF. Connections of the auditory brainstem in a songbird, *Taeniopygia guttata*: III. Projections of the superior olive and lateral lemniscal nuclei. J Comp Neurol. 2010; 518:2149–2167. [PubMed: 20394063]

Wong-Riley M. Changes in the visual system of monocularly sutured or enucleated cats demonstrable with cyto-chrome oxidase histochemistry. Brain Res. 1979; 171:11–28. [PubMed: 223730]

Woolley SM, Casseday JH. Response properties of single neurons in the zebra finch auditory midbrain: response patterns, frequency coding, intensity coding, and spike latencies. J Neurophysiol. 2004; 91:136–151. [PubMed: 14523072]

Woolley SM, Casseday JH. Processing of modulated sounds in the zebra finch auditory midbrain: responses to noise, frequency sweeps, and sinusoidal amplitude modulations. J Neurophysiol. 2005; 94:1143–1157. [PubMed: 15817647]

Woolley SM, Rubel EW. Bengalese finches Lonchura Striata domestica depend upon auditory feedback for the maintenance of adult song. J Neurosci. 1997; 17:6380–6390. [PubMed: 9236246]

Zeng SJ, Lin YT, Yang L, Zhang X-W, Zuo M-X. Comparative analysis of neurogenesis between the core and shell regions of auditory areas in the chick (Gallus gallus domesticus). Brain Res. 2008; 1216:24–37. [PubMed: 18486109]

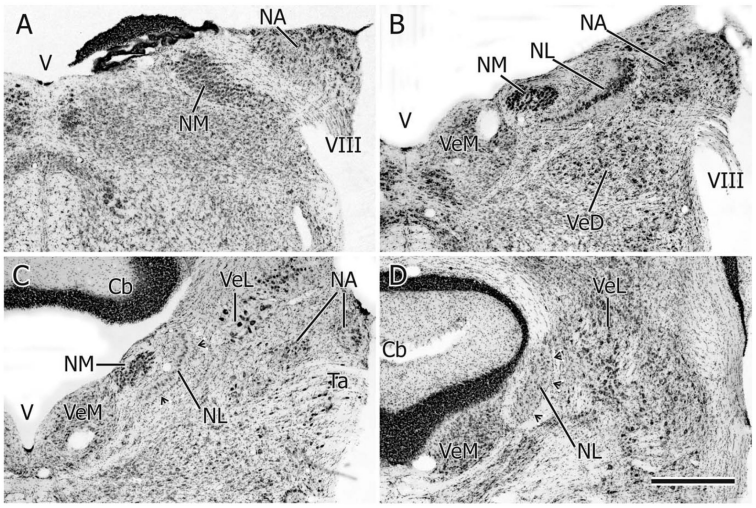

Figure 1.

A–D: Transverse sections (35 μm thick) at four rostrocaudal levels through the cochlear nuclei (NA, NM) and NL, A being most caudal and D most rostral. Cresyl violet stain. Cb: cerebellum; Ta: tangential nucleus; V: 4th ventricle; VeD: descending vestibular nucleus; VeL: lateral vestibular nucleus; VeM: medial vestibular nucleus; VIII: vestibulocochlear nerve. Arrowheads in C and D point to the wall of glia on the lateral aspect of NL. Scale bar = 500 μm.

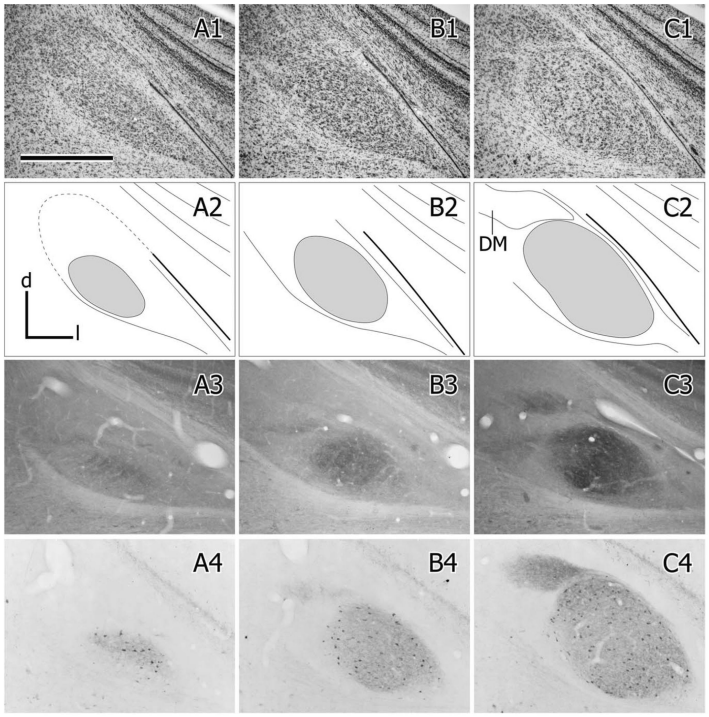

(a)

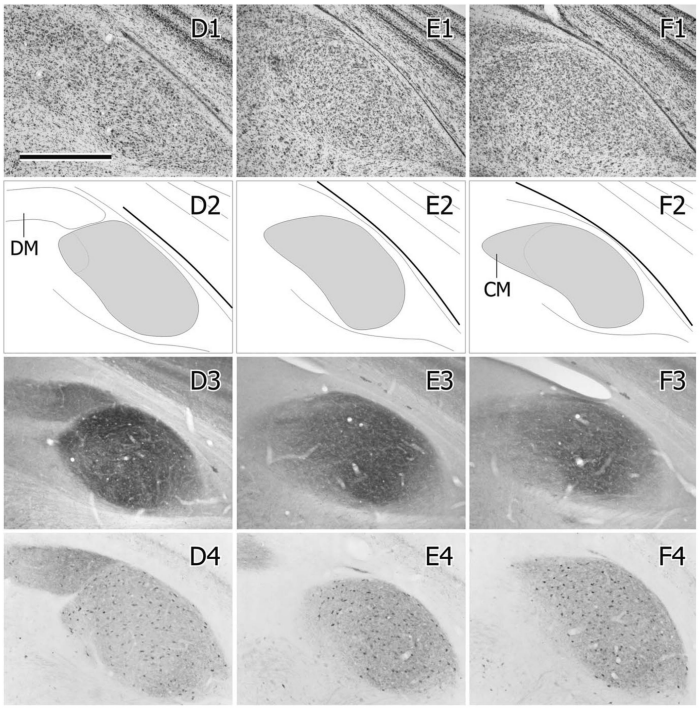

(b)

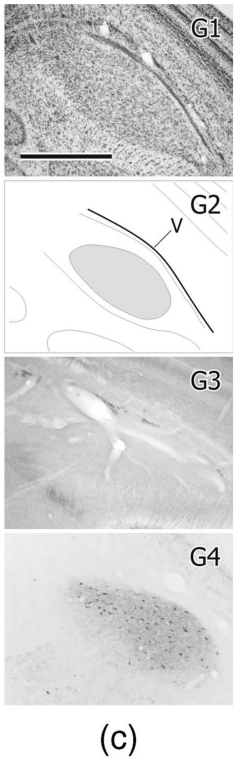

Figure 2.

A1–G1: A caudal to rostral series of cresyl violet counterstained transverse sections through the right MLd; dorsal is up, lateral to the right. **A2–G2:** Schematic outlines of the sections shown in A1–G1. MLd is gray; DM is the dorsomedial nucleus of the intercollicular region; CM is the caudomedial nucleus (Puelles et al., 1994; Wild, 1995); V is the tectal ventricle. **A3–G3:** Cytochrome oxidase stained sections from a different brain at roughly corresponding levels to those in A1–G1. **A4–G4:** Parvalbumin immunolabeled sections from the same brain shown in A1–G1. Scale bars = 500 μm.

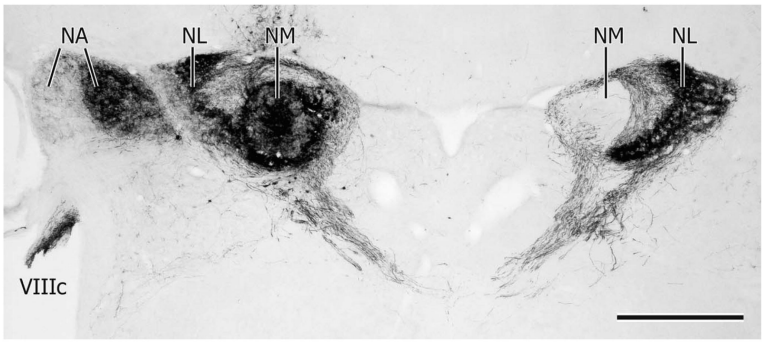

Figure 3.
Noncounterstained transverse section through NA, NM, and NL at a caudal level showing an injection of BDA centered on the left NM. Note 1) retrogradely labeled fibers in the ipsilateral cochlear part of the eighth nerve (VIIIc) and terminal labeling in the medial part of NA; 2) dense anterograde labeling of NM projections to NL bilaterally; 3) the absence of retrogradely labeled cell bodies in the right NM at this level (see text). Scale bar = 500 μm.

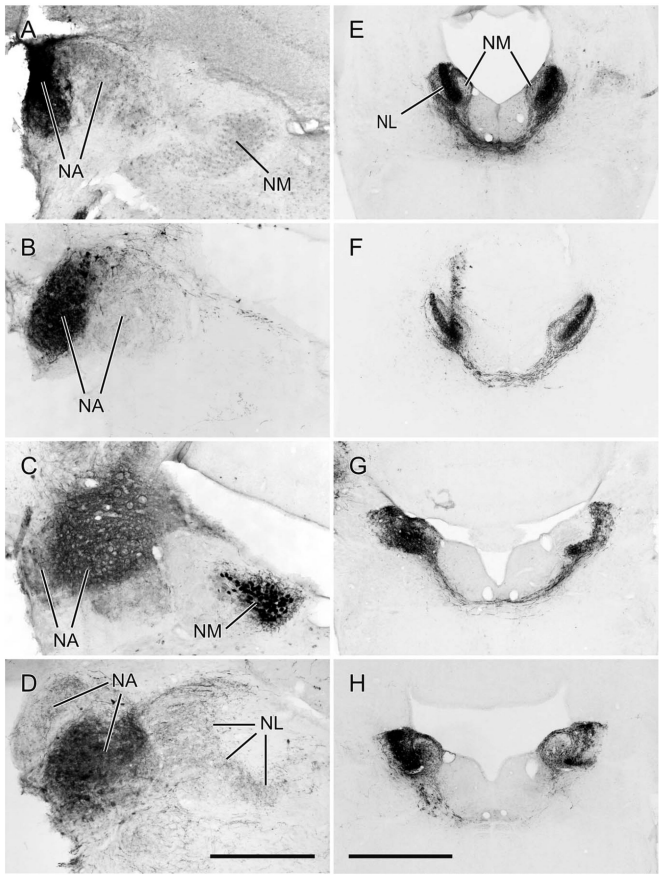

Figure 4.

A–D: Examples of typical injections in NA. A,B: Injections of BDA confined to the lateral part of NA at a caudal and a slightly more rostral level, respectively. C,D: Injections of CTB in the medial part of NA, C being at approximately the same level as B and D at a similar level to A. C also shows retrogradely labeled cell bodies in NM resulting from an injection of BDA in the contralateral NL in the same case. **E–H:** Injections of BDA in different parts of the left NL in each case. Note that in each case both the left and the right NL are anterogradely labeled as a result of somatopetal and somatofugal transport to and from NM. Noncounterstained transverse sections. Scale bars = 400 μm for NA cases and 1 mm for NL cases.

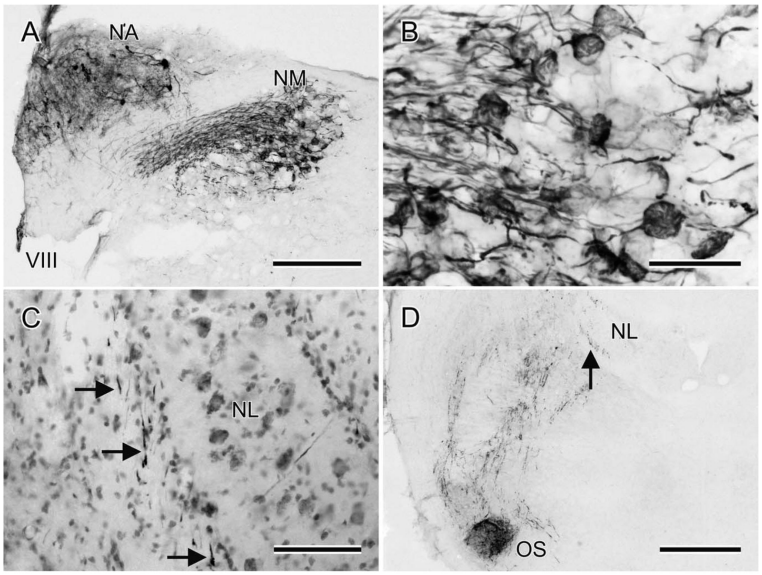

Figure 5.

A: The results of an injection of BDA in the left NA at a more rostral level. In NA there is diffusion of BDA and some retrogradely labeled cell bodies, the axons of which presumably travel rostrally, through the injection site. Ventromedial to NA there are labeled processes in the eighth nerve root and their calyceal terminations on NM cell bodies, shown at higher power in **B. C:** BDA-labeled NA axons (at the arrows) adjacent to the lateral border of the ipsilateral NL, Nissl counterstain. **D:** BDA-labeled processes coursing as several swaths through the tegmentum between an injection in NA at a more caudal level and OS. Most of these processes are NA projections to OS and beyond, but some could be the axons of retrogradely labeled OS neurons. As in C, note the fiber labeling (at the arrow) on the lateral aspect of NL. Scale bars = 250 μm in A; 50 μm in B; 100 μm in C; 500 μm in D.

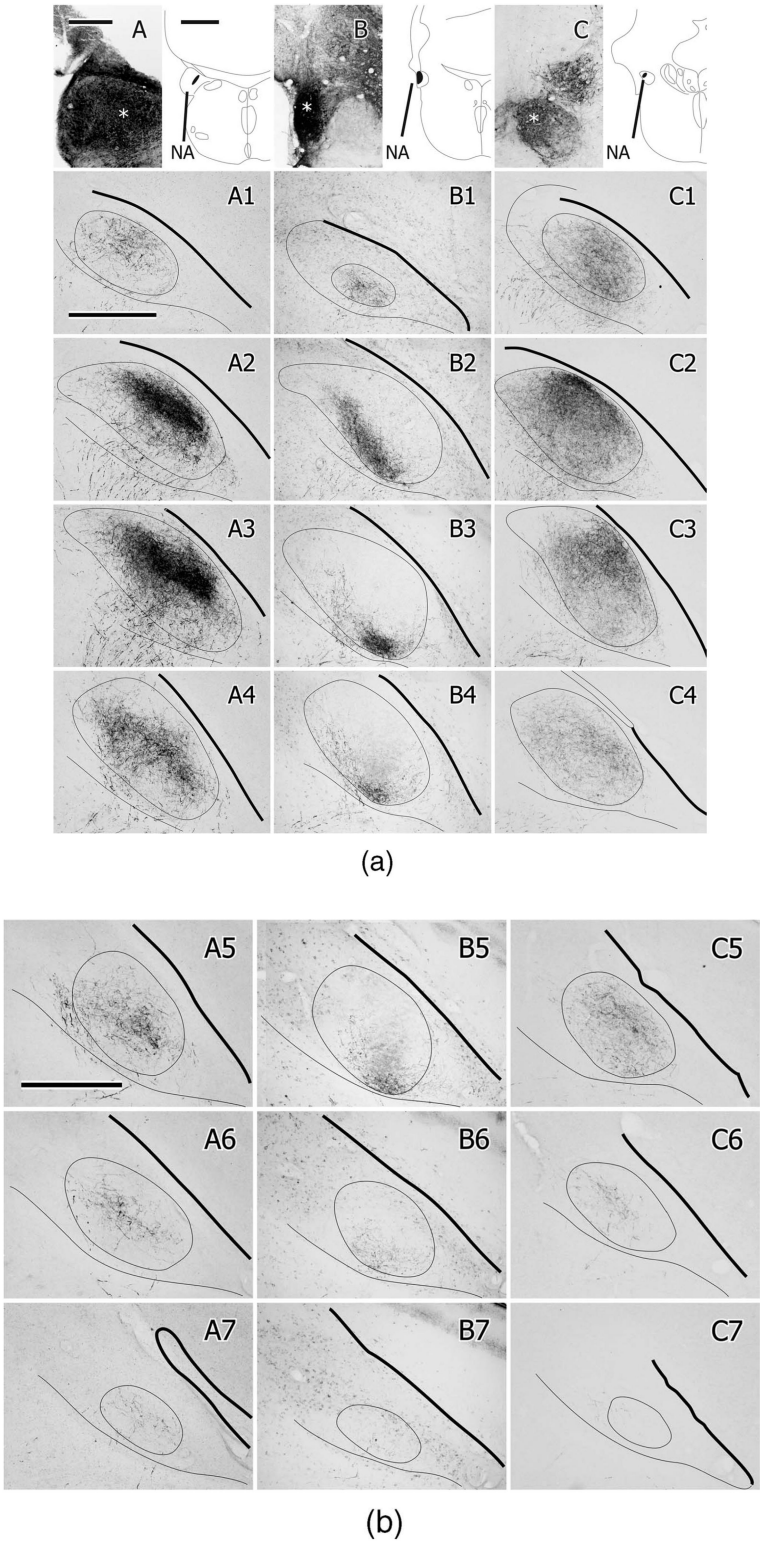

Figure 6.

A–C: Injections of BDA in different parts of the left NA in three different cases, the location of which is shown in the schematic section outlines. The asterisks depict the center of the

injection in each case. **A1–A7,B1–B7,C1–C7:** Caudal to rostral series of projections to the contralateral (right) MLd for each case. Each box depicts the labeled fibers and terminations imaged in three of four consecutive, noncounterstained, 35-μm-thick sections and projected onto an outline of MLd drawn from a middle one of the four. One of the four sections was counterstained but did not contribute to the labeling. The thick line represents the overlying tectal ventricle, the thin line under MLd represents the ventral border of the intercollicular complex. Scale bars = 250 μm for A–C; 1 mm for schematics; 500 μm for A1–C7.

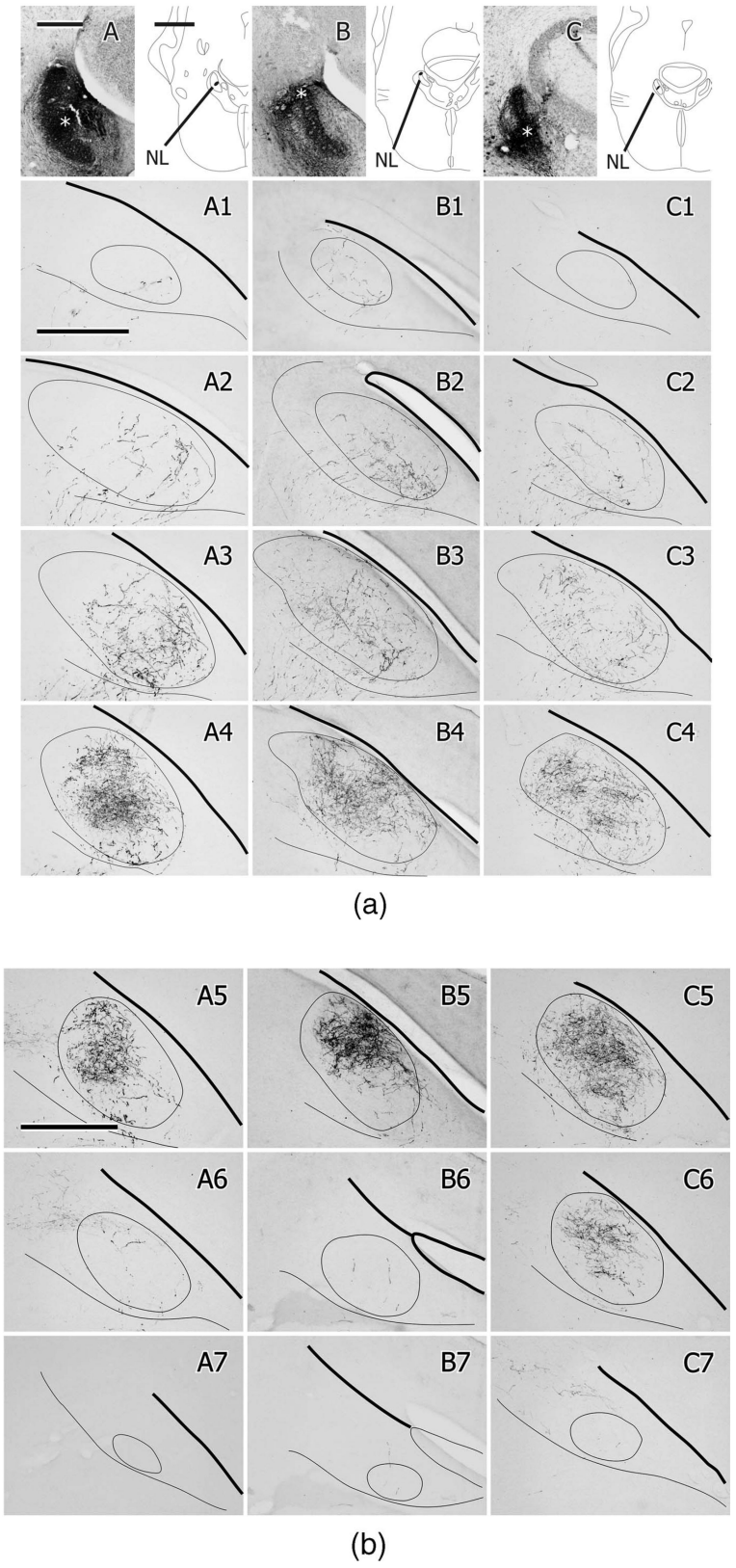

Figure 7.

A–C: Injections of BDA in different parts of the left NL in three different cases, the location of which is shown in the schematic section outlines. The asterisks depict the center of the injection in each case. **A1–A7,B1–B7,C1–C7:** Caudal to rostral series of projections to the contralateral (right) MLd for each case. Each box depicts the labeled fibers and terminations imaged in three of four consecutive, noncounterstained, 35-μm-thick sections and projected onto an outline of MLd drawn from a middle one of the four. One of the four sections was counterstained but did not contribute to the labeling. The thick line represents the overlying tectal ventricle, the thin line under MLd represents the ventral border of the intercollicular complex. Scale bars = 250 μm for A–C; 1 mm for schematics; 500 μm for A1–C7.

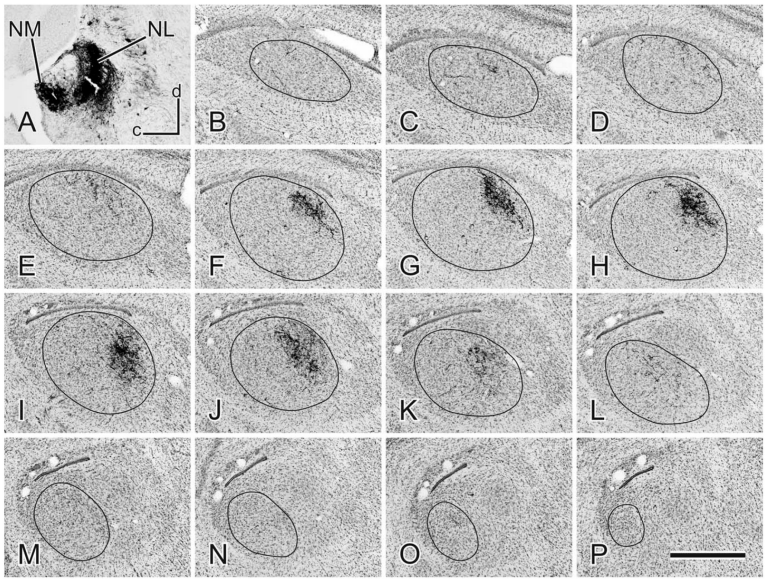

Figure 8.

An example of a BDA injection in NL **(A)** and the projections throughout the contralateral MLd seen in a medial to lateral **(B–P)** series of sagittal, cresyl violet counterstained sections. Dorsal (d) is up and caudal (c) is left. Scale bar = 500 μm.

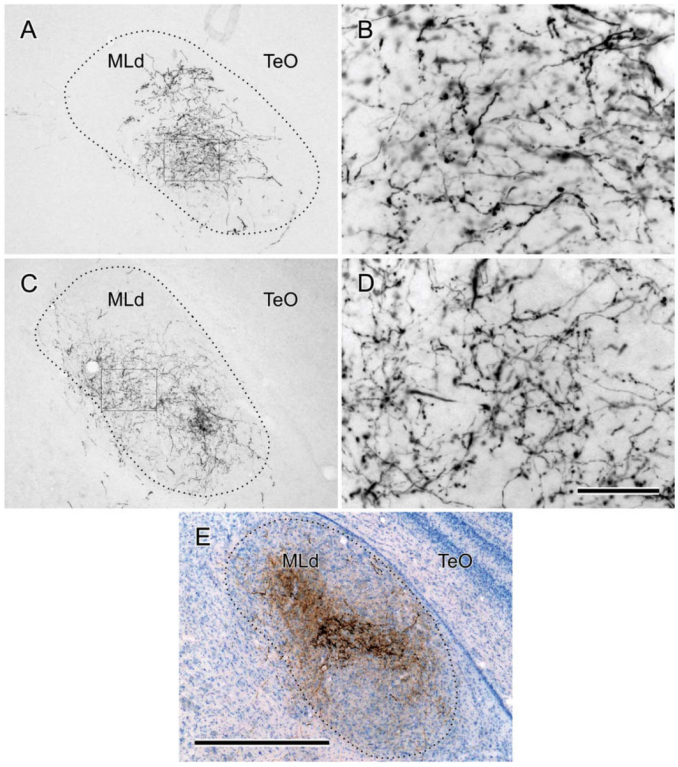

Figure 9.

A–D: Photomicrographs showing fiber and terminal labeling in the right MLd following injections of BDA in the left NL (A,B) or left NA (C,D). B,D: Higher-power views of the areas boxed in A,C, respectively. **E:** Photomicrograph of a single, 35-μm, counterstained, transverse section through MLd showing fiber and terminal labeling resulting from a case receiving a BDA injection in NL (black label) and a CTB injection in NA (brown label) on the same side. Scale bars = 500 μm for A,C,E; 50 μm for B,D.

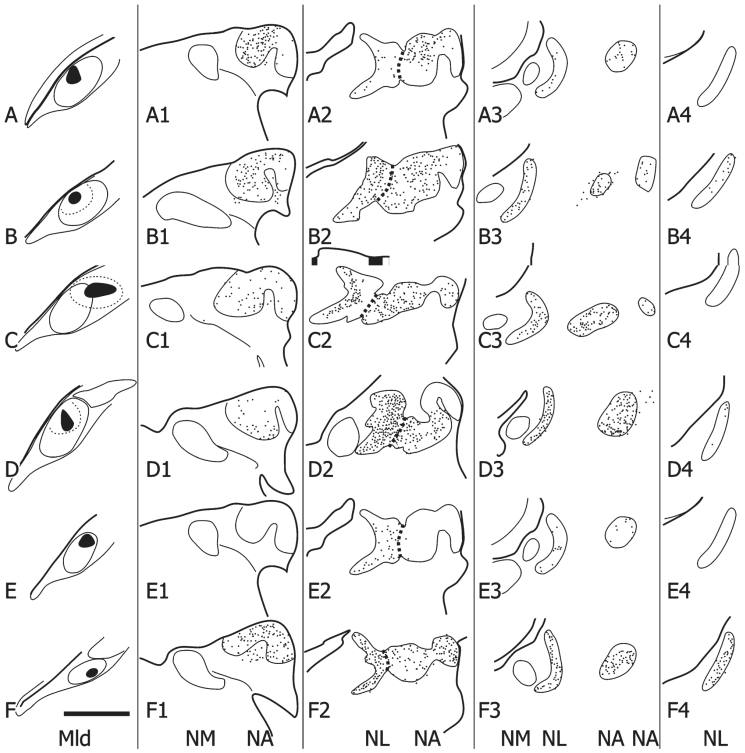

Figure 10.

A1–A4,B1–B4…**F1–F4:** Schematic depictions of the location and number of retrogradely labeled cell bodies in single, 35-μm-thick sections through the right NA and NL at four different rostrocaudal levels (the second column being the most caudal and the last column at right the most rostral) resulting from six injections of either CTB (A–D,F) or BDA (E) in the contralateral (left) MLd (one case received two injections, one of CTB (A) and the other of BDA (E)). The injections are shown as solid black in the first column and the labeled cells as dots in the next four columns. The short dashed lines depict the border between NA and NL. Scale bar = 500 μm.

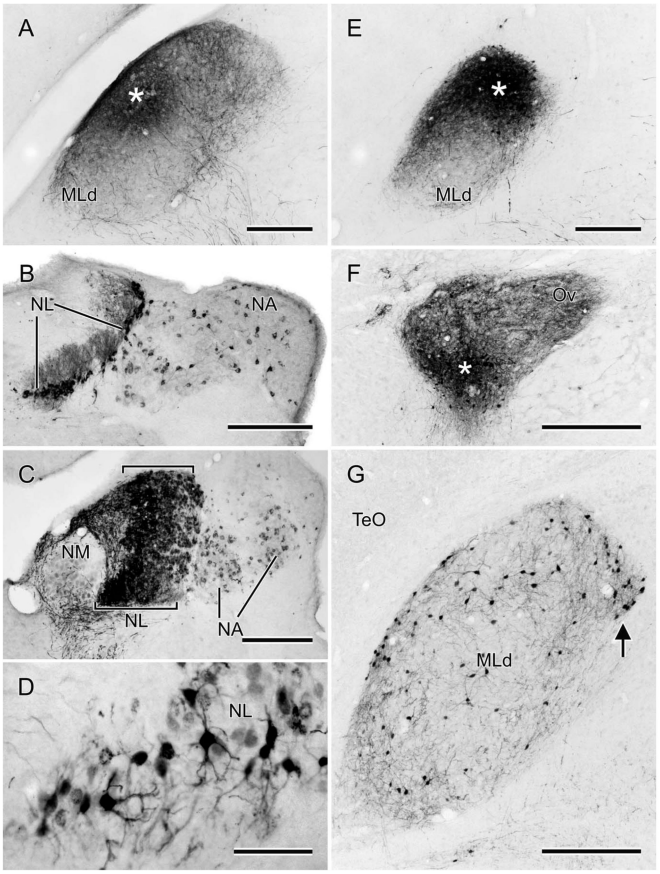

Figure 11.

A,E: Photomicrographs of the MLd injections of CTB (A) or BDA (E) (asterisks depict the injection centers) that produced the retrogradely labeled cells in NA and NL depicted in Fig. 10A,E, respectively. **B:** Retrogradely labeled cells in the right NL and medial and lateral parts of NA, resulting from the injection shown in Fig. 10C. Note the labeling of NL dendrites, particularly on the medial (internal) aspect of the nucleus at this level. **C:** Retrogradely labeled cell bodies in NL and medial and lateral NA, resulting from the injection of CTB depicted in Fig. 10D. Note the width of NL at this level (between brackets). **D:** Retrogradely labeled cells in NL resulting from the injection of BDA shown in Figs. 10E and 11E. **F:** An iontophoretic injection of BDA in the ventral part of the left Ov, asterisk marks its center. **G:** Retrogradely labeled cells in the ipsilateral MLd resulting from the injection in F. Note the cluster of labeled cells at the ventromedial corner of the nucleus (arrow); see text for normal anatomy of MLd. Scale bars = 250 μm for A–C,E; 75 μm for D; 500 μm for F; 350 μm for G.